

## TX Cancri—Which Component is Hotter?

Robert E. Wilson

Institute for Space Studies Goddard Space Flight Center, New York  
Department of Astronomy University of South Florida,  
Department of Physics and Astronomy University of Florida

Peter Biermann

Astronomische Institute der Universität Bonn

Received October 23, 1975

**Summary.** We raise the question of whether the W-type light curves (occultation primary eclipse) of TX Cnc are due to the low mass component being slightly the hotter component, as presumed until now, or whether it might be due to TX Cnc having the relatively strong classical gravity darkening law. To decide this question, we have analysed TX Cnc light curves from four “epochs” showing dissimilar behavior. Two of these epochs appear (almost) reasonably normal, while the other two are very abnormal. The analysis was done in two different modes—one with the second temperature a free parameter, as in Whelan *et al.* (1973), and one with the second temperature determined by the first temperature and the surface gravity as in Wilson and Devinney (1973). We prefer the latter approach for two reasons, which are discussed in the paper. We find that the polar effective temperature of the low mass star is then about 30 °K cooler than that of the high mass star, compared to values of 125 to 175 °K hotter under the “T 2 free parameter” approach. Thus we find

no evidence for a significant difference in the adiabatic constants of the two convection zones. TX Cnc is the second contact binary, after RZ Com, for which a gravity darkening explanation adequately accounts for a W-type light curve. In regard to the mass ratio and inclination, our results are in good agreement with those of Whelan *et al.*, but we find a significantly smaller geometrical overcontact. Epoch to epoch changes in the gravity darkening and albedo parameters suggest differences in the degree of *thermal* contact over the time scale of a few years. Some accuracy-related improvements in the Wilson-Devinney light curve and differential corrections procedures are described. Also, a scheme is given for ensuring convergence in differential corrections solutions in the presence of high correlations involving many parameters.

**Key words:** contact binaries — W UMa binaries — TX Cancri

### I. Introduction

TX Cancri is a binary of the W UMa class and is of special interest since it is in the cluster Praesepe and thus has a known distance, absolute magnitude and age. It was discovered by Haffner (1937), and discussed by Hazlehurst (1970), Yamasaki and Kitamura (1972), Biermann and Thomas (1973) and Whelan *et al.* (1973; hereafter WWM). Hazlehurst (1970) considered TX Cnc a puzzle since he was unable to make zero age models, whereas TX Cnc, being several magnitudes below the cluster turnoff, must be close to age zero. Biermann and Thomas (1973) produced models for TX Cnc and similar binaries with a model (cf. Lucy, 1968a) that has different adiabatic constants in the two convection zones around the two components. However they were unable to reproduce the light curves adequately. WWM analysed new observations and constructed a model that reproduces all observed properties including the

light curve. In order to do this, however, they had to push the region of energy exchange to highly super-adiabatic levels, which is not comprehensible on physical grounds. This point kept Biermann and Thomas from constructing such models, which are an extension of their Table 1.

Thus no acceptable model for TX Cnc exists and we are back to the puzzling conclusion of Yamasaki and Kitamura (1972) who found it difficult to understand the system with any theoretical model. More progress at this stage may be expected from consideration of the large body of observations.

In this paper we consider the following main question in regard to TX Cnc: Is the component of lower mass the hotter one, as found by WWM? Although this point concerns temperature differences of only a few hundred degrees, it places an important constraint on structural

models, if true. Furthermore, it has become virtually an accepted fact (Whelan, 1972; Hazlehurst and others, private communication) that the low mass star is the hotter one for all W UMa systems which show W-type light curves, such as TX Cnc. However, on the basis of our results below, it seems that TX Cnc is a counter-example. According to Wilson and Devinney (1973), RZ Comae is also a counter-example.

Here we derive photometric parameters for TX Cnc, using observations by Kitamura and Yamasaki (1971; hereafter KY), and by WWM. The least squares differential corrections program has been described by Wilson and Devinney (1971; 1973), and by Wilson *et al.* (1972). We do the analysis for up to five colors rather than one, as WWM and thus hope to improve the reliability of the results. Second, we do the analysis for four different epochs, rather than one, as WWM and can thus check on temporal variations of parameters connected with the energy exchange, such as the temperature difference, the gravity darkening exponent, and the bolometric albedo. This is of interest because the thermal timescales of the surface layers can be as low as a few years (Biermann and Thomas, 1973). Furthermore Lucy (1975) recently suggested that small oscillations might be the hallmark of the energy exchange. Finally we do the solutions in two different “modes”—one with the temperature difference between components a free parameter, as in WWM, and one with the temperature difference determined by the surface gravity field, as in Wilson and Devinney, 1973. These modes are discussed more fully in the next section.

## II. Procedural Improvements

One of the main points of divergence in recent papers on models for contact binaries concerns the presence or absence of a discontinuity, or region of rapid transition in surface effective temperature, at the narrow neck connecting the components. While the issue is not usually posed in terms of such a discontinuity, it is implicit in the procedures adopted by various authors. For example, Lucy (1968b) and Wilson and Devinney (1973) tacitly excluded such a discontinuity, the former because he made no distinction between one component and the other so far as the surface is concerned, and the latter by constraining  $T_2$  (polar) to have just that value which, given  $T_1$  (polar), causes the discontinuity to vanish. On the other hand WWM allowed  $T_2$  to be a free parameter, to be chosen so as to give agreement with the observed light curve, so that in general such a discontinuity is expected. This follows from the fact that local effective temperature is given by a law of the form

$$T_{\text{local}} = T_{\text{r.p.}} \left( \frac{a_{\text{local}}}{a_{\text{r.p.}}} \right)^{0.25g} \quad (1)$$

where we call  $g$  the “gravity darkening exponent”,  $a$  is the local acceleration due to gravity, and r.p. stand for “reference point” (usually the pole of one component). Since all authors adopt only one value of  $g$  for the entire surface of a given contact binary, Eq. (1) contains no further free parameters except the temperature of the reference point, and thus specifies  $T_2$  (polar) as soon as  $T_1$  (polar) is given, for a given choice of  $g$ . The treatment of  $T_2$  as a free parameter by WWM, is thus equivalent to the introduction of a scaling factor between separate laws of the form (1) for each component, so that a discontinuity in surface effective temperature will necessarily result at the boundary which separates the components.

It now seems clear that the question of whether  $T_2$  should be regarded as a free parameter in analyzing the observations of normal WUMa type stars is a matter to be approached with some caution, especially since it has important consequences for the theory of their structure. Thus a new mode of operation has been added to the basic light curve and differential corrections programs by Wilson and Devinney (1971), in which all the constraints otherwise applied to contact binary cases are applied *except* that on  $T_2$ . That is the new mode (mode 3) sets

$$g_2 = g_1 \quad (\text{gravity darkening})$$

$$A_2 = A_1 \quad (\text{albedo})$$

$$\Omega_2 = \Omega_1 \quad (\text{surface potential}) \text{ and}$$

$$x_2 = x_1 \quad (\text{limb darkening})$$

but *not*

$$T_2 = T_1 (a_2/a_1)^{0.25g},$$

as in the other contact binary mode (mode 1). The new mode makes it possible to repeat the analysis of TX Cnc by WWM<sup>1)</sup> but now with the temperature difference between components found by simultaneous solution of light curves in all measured passbands rather than the  $V$  passband alone. Of course the older mode (1) can also be used, so we shall be in a position to judge whether or not the extra degree of freedom provided by the parameter  $T_2$  significantly improves the agreement with the observations.

Since we are concerned here with temperature differences of at most a few hundred degrees between temperatures of the order of 6000 °K, good internal consistency and overall accuracy of the basic computing scheme are very important. Several accuracy-related improvements were made before treating TX Cnc. One of these provides the option of computing symmetrical derivatives (i.e. the finite difference equivalent of a Schwarz derivative) rather than asymmetrical numerical derivatives. The asymmetric “derivatives” are de-

<sup>1)</sup> There is, however, one difference: They adopted a fixed value for  $g$ , whereas we treat  $g$  as a free parameter to be determined from the data.

fined by

$$\frac{\partial l}{\partial p} = \frac{l(p + \Delta p) - l(p)}{\Delta p}$$

as before, while the symmetric “derivatives” are defined by

$$\frac{\partial l}{\partial p} = \frac{l(p + \Delta p/2) - l(p - \Delta p/2)}{\Delta p},$$

where  $p$  is any model parameter. Experience shows that the use of symmetric derivatives makes negligible changes in the solutions for TX Cnc, but it is reassuring to know this, and the option is now available for future use. Symmetric derivatives require about 1.8 times as much computing time as asymmetric derivatives.

In the original program, the boundary between the components of a contact binary was taken to be the intersection with the common envelope of a plane normal to the line of centers which passes through the inner Lagrangian point. However it happens that the minimum “neck” diameter does not coincide exactly with this plane, but in general is displaced slightly toward the less massive component. Neglect of this apparently rather fine point will result in a loss of computing accuracy for the lower mass component because the region around the “hole” near the  $L_1$  point turns slightly outward like the mouth of a trumpet. As a result, the local surface elements, which are most conveniently spaced at equal *angular* intervals, became rather large, and this condition leads to a major increase in quantizing error as these areas are clipped off at the boundary. We now eliminate this problem by placing the boundary ring actually at the neck minimum rather than at the  $x$ -coordinate of the  $L_1$  point. This is accomplished by a subroutine (called NEKMIN) which computes the  $x, z$  coordinates corresponding to minimum neck diameter. The ring around the minimum in the neck is not precisely a plane curve since the minimum occurs at a slightly different  $x$ -coordinate in the  $x, y$  plane than in the  $x, z$  plane. For definiteness, therefore, we adopt the  $x, z$  plane, in the equation which defined the surface of our common envelope (Kopal, 1959; Wilson and Devinney, 1971). Expressed in rectangular coordinates, it then becomes

$$\Omega = \frac{1}{\sqrt{x^2 + z^2}} + \frac{q}{\sqrt{(1-x)^2 + z^2}} + \frac{(q+1)}{2}x^2 - qx. \quad (2)$$

Since two coordinates are to be found, a second condition is needed, and this, of course, is that  $\partial\Omega/\partial x=0$ , since we are to find a minimum in the surface. We have, therefore,

$$\frac{\partial\Omega}{\partial x} = -\frac{x}{(x^2 + z^2)^{3/2}} + \frac{q(1-x)}{[(1-x)^2 + z^2]^{3/2}} + (q+1)x - q = 0. \quad (3)$$

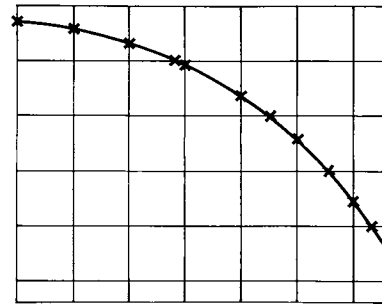


Fig. 1. Schematic representation of a section of grid elements as viewed from the inside of one component. Vertical and horizontal lines are lines of constant longitude and latitude, respectively. The curve is part of the boundary ring, by which we separate components 1 and 2. Crosses mark the intersections of the coordinate grid with the boundary ring

We can find  $x, z$  from Eqs. (2) and (3) in an iterative way by solving the two simultaneous equations

$$\Omega_{in} - \Omega = \frac{\partial\Omega}{\partial x} \Delta x + \frac{\partial\Omega}{\partial z} \Delta z \quad (4)$$

and

$$-\frac{\partial\Omega}{\partial x} = \frac{\partial^2\Omega}{\partial x^2} \Delta x + \frac{\partial^2\Omega}{\partial z\partial x} \Delta z, \quad (5)$$

where (4) is the condition to be on the surface and (5) is the condition for a minimum neck radius. The quantities  $\Delta x, \Delta z$  are corrections to the  $x, z$  values of the previous iteration. Finally, we list the three remaining derivatives

$$\frac{\partial^2\Omega}{\partial x^2} = \frac{2x^2 - z^2}{(x^2 + z^2)^{5/2}} + \frac{q[2(1-x)^2 - z^2]}{[(1-x)^2 + z^2]^{5/2}} + (q+1) \quad (6)$$

$$\frac{\partial\Omega}{\partial z} = -\frac{z}{(x^2 + z^2)^{3/2}} - \frac{qz}{[(1-x)^2 + z^2]^{3/2}} \quad (7)$$

$$\frac{\partial^2\Omega}{\partial z\partial x} = \frac{3xz}{(x^2 + z^2)^{5/2}} - \frac{3qz(1-x)}{[(1-x)^2 + z^2]^{5/2}}. \quad (8)$$

Quantizing error due to the “clipping off” of surface elements by the boundary ring is now dealt with in a more effective way than originally. Figure 1 is a schematic representation of a short arc of the boundary ring as it intersects the surface of the common envelope, with the view from the inside of the star. While the visual impression is that of rectangles marked on a surface, we are really most basically concerned with the solid angles subtended at the center of the star by these “rectangles” and, in fact, the solid angles define the surface areas (not the other way around). In order to correct for quantizing effects, we multiply the local contributions to luminosity and line-of-sight flux by a function  $F$ , defined so as to correct for fractional area effects. Table 1 summarizes the exact way in which  $F$ , and an intermediary function,  $f$ , are defined.

Table 1

Case	Values of $F, f$
I. Center of elemental area (e.a.) inside boundary ring	$F = 0.$ $0 \leq f \leq 0.5$
II. Entire e.a. outside boundary ring	$F = 1$ $f = 1$
III. Center of e.a. outside ring, but part of e.a. inside ring	$F = f$ $0.5 \leq f \leq 1.0$
IV. Special case of first e.a. with center outside boundary ring. $k$ is running e.a. number on latitude row, $n$ is number of first e.a. with center outside boundary ring.	$F = \sum_{k=1}^n f_k$ $0.5 \leq f_n \leq 1.0$ $0. \leq f_k \leq 0.5$ for $1 \leq k < n$

The function  $f$  is the fraction of an elemental area which lies *outside* the boundary (i.e. the fraction which *should* be counted.) However we do not wish to work with an elemental area whose center lies “in the hole” for obvious reasons. Therefore we assign all fractional areas associated with such elements to the first elemental area whose center lies outside the hole (case IV). The values of  $f$  are obtained by actually locating the latitude and longitude ( $\theta, \phi$ ) of each intersection between the boundary ring and the sides of the elemental areas. These intersections are marked by crosses in Fig. 1. At present, we make the approximation that these intersections are connected by straight lines in computing  $f$ . One could make them arcs of circles, but that refinement seems unnecessary, at present. The analytic techniques and logic schemes by which the intersections are found are much too extensive to be given here, but if significant interest in these matters should arise, we might write up a description for private circulation. However, the computing time required is not very great and is negligible compared to that for the light curve or differential corrections program as a whole.

### III. Differential Corrections Solutions

The observations of TX Cnc by KY show changes in the form of the light curve with time, and the light curve by WWM is different from any of those by KY.

Table 2. Definition of Epochs

Epoch	Dates of Observation	Passbands Included	Reference
I	1962, Dec. 12, 13 1965, Nov. 30, Dec. 21 1966, Jan. 15, 17, 27, Feb. 17	$V, B, U$ $\lambda 4870,$ $\lambda 4110$	KY
II	1965, Jan. 13, 14	$V, B$	KY
III	1971, Feb. 4, 5	$V, B$	KY
IV	1972, Jan. 13–16, Feb. 12–14	$V$	WWM

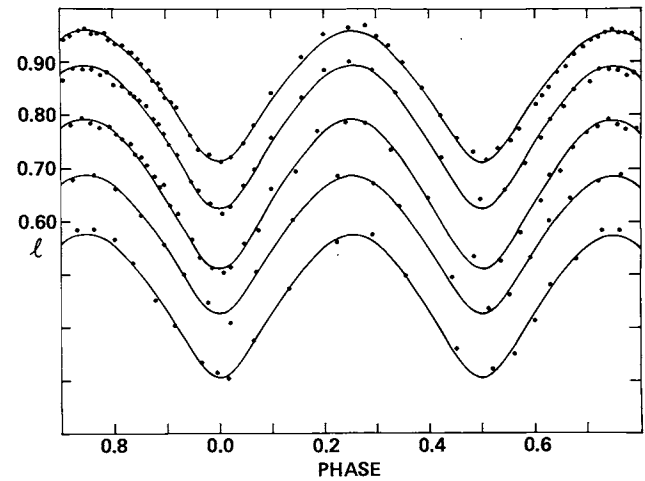


Fig. 2. The light curves of epoch I by KY and our mode 1 solution curves. From top to bottom the passbands are  $V, B, U, \lambda 4870$  narrow band and  $\lambda 4110$  narrow band. Notice the asymmetries in the observations. The vertical scale numbers apply directly for the uppermost curve. For the second curve, add 0.10 to the numbers; for the third 0.20, etc.

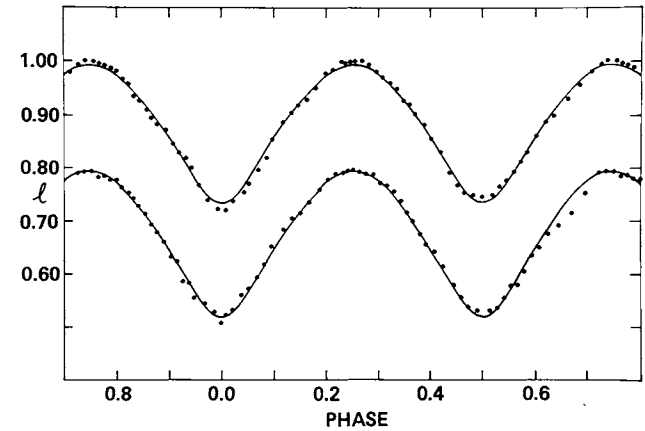


Fig. 3. The light curves of epoch II by KY and our mode 1 solution curves in  $V$  (top) and  $B$ . This is the epoch treated by WWM. The asymmetries are somewhat different from those of epoch I, but otherwise the curves are similar to epoch I. Notice that the bottom of secondary eclipse is fitted poorly, as was also the case in WWM. The vertical scale comments for Fig. 2 apply here also

Although the differences amount to a few hundredths of a magnitude only, they are unquestionably real and may give clues to the nature of the energy exchange. However the changes are not secular (similar light curves return) so we have grouped the data into four “epochs” according to light curve similarities, as defined by Table 2.

Note that epochs II, III and IV cover fairly brief intervals of time, but that “epoch” I is a blend of several true epochs at which the light curve appeared essentially the same to visual inspection. Note also that these sub-epochs of epoch I bracket epoch II in time. Normal points of the observations for epochs I, II and III, and the individual observations of epoch IV are shown in Figs. 2–5.

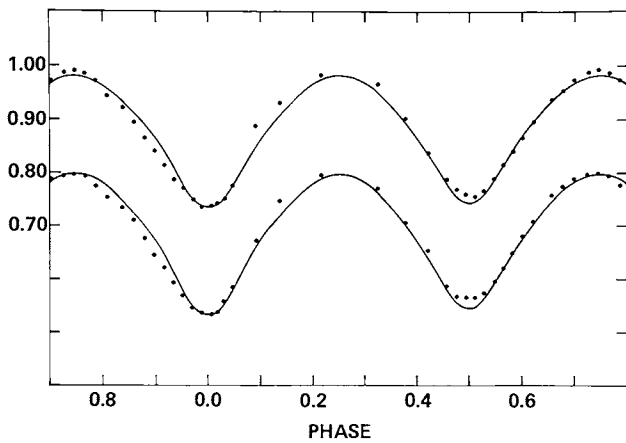


Fig. 4. The light curves of epoch III by KY and our mode 1 solution curves in  $V$  (top) and  $B$ . The asymmetries are now very large. The vertical scale comments for Fig. 2 apply here also

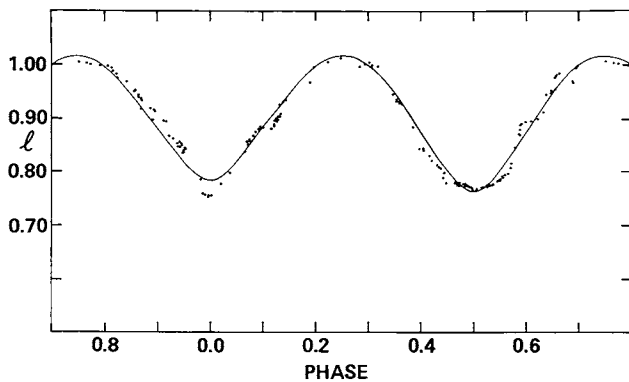


Fig. 5. The  $V$  light curve of epoch IV by WWM and our mode 1 solution curve. The general shape of the light curve is conspicuously different from that of a normal W UMa system at this epoch

At this point we encounter the first of two problems with parameter correlations. It is well known that strong correlations exist among the parameters of eclipsing binary solutions, and we have confirmed this by computing and printing the matrix of correlation coefficients with each solution, as a matter of routine. We find that the correlations are especially strong for contact binaries. Now the object of treating four separate epochs of observations is to detect real temporal changes in the binary system, but if we solve for all parameters at all epochs we can expect difficulty in deciding how much of an apparent change in, say, bolometric albedo, is real and how much is due to correlations with other quantities, such as the inclination. Therefore we solved for the full set of elements only at epoch I and, at the other three epochs, solved only for *those elements which might reasonably be expected to vary with time*. Thus, at epochs II, III and IV, we implicitly accept a certain (hopefully small) amount of systematic error in the derived parameters, which is due to the imposition of fixed values for selected parameters, in order to obtain meaningful *epoch-to-*

Table 3. Parameters Not Adjusted<sup>a)</sup>

$T_1$	6400 °K	$r_1$ (pole)	$0.317 \pm .002$ p.e. $0.318 \pm .002$
$x(V)$	0.66	$r_1$ (side)	$0.331 \pm .003$ $0.333 \pm .003$
$x(B)$	0.79	$r_1$ (back)	$0.365 \pm .005$ $0.368 \pm .004$
$x(U)$	0.84		
$x(\lambda 4870)$	0.72	$r_2$ (pole)	$0.401 \pm .002$ $0.404 \pm .002$
$x(\lambda 4110)$	0.82	$r_2$ (side)	$0.425 \pm .003$ $0.428 \pm .003$
$\Omega$ inner contact	4.7649 4.7883		
$\Omega$ outer contact	4.1800 4.2027	$r_2$ (back)	$0.455 \pm .004$ $0.459 \pm .004$

<sup>a)</sup> Where two entries are given, the upper is for the mode 1 solution, the lower for the mode 3 solution.

Here  $T_1$  is the effective temperature at the pole of component 1,  $x(U)$ ,  $x(B)$  and  $x(V)$  are the limb darkening coefficients,  $\Omega$  the Roche modified potential at the inner and outer contact points (the surface potential of the stars must lie between the two values for a contact binary),  $r_1$  and  $r_2$  the radii of the two stars in the respective directions in units of the distance between the centers of gravity of the two components.

*epoch differences* for other parameters in a simple and direct way. All fixed and adjusted parameters are listed in Tables 3 and 4.

Naturally it is the temperature difference between components and not the individual temperatures which are interesting in Table 4. For reasons of convenience we have kept  $T_1$  fixed (at 6400 °K) and allowed  $T_2$  to adjust, rather than the other way around. If users of these results prefer to keep  $T_2$  (i.e. that of the more massive and more luminous component) fixed and allow  $T_1$  to be variable, or if they prefer a reference temperature other than 6400 °K, simple and obvious scaling procedures can be applied without affecting the other parameters of Table 4.

The solutions for the full parameter set were done at epoch I because it contains data in five passbands, compared to two in epochs II and III and one in epoch IV. It is well known that attempts to solve for too many parameters will weaken a solution, so we inserted theoretical values for the limb darkening coefficients, and these were not adjusted. The limb darkening values (viz. Table 3) were extracted from tables by Carbon and Gingerich (1969). For epoch I we solved for the orbital inclination ( $i$ ), gravity darkening exponent ( $g=4\beta$ ), polar temperature of the photometric secondary, or mass primary ( $T_2$ ), bolometric albedo ( $A$ ), surface modified potential ( $\Omega$ ), mass ratio ( $q=M_2/M_1$ ), and relative luminosity of the photometric primary ( $L_1$ ), which includes the scaling factor needed to match the observed light values. Only the luminosity *ratio* has physical significance in analysis of light curves, so we list only the quantity  $[L_1/(L_1+L_2)]$  in Table 4. For the other three epochs, we kept  $i$ ,  $\Omega$  and  $q$

Table 4. Adjusted Parameters<sup>a)</sup>

param. \ Epoch	I	II	III	IV
$i$	$62.43 \pm .33$ p.e.	...	...	...
	$62.84 \pm .28$	...	...	...
$g$	$0.88 \pm .12$	$1.02 \pm .03$	$0.69 \pm .06$	$0.32 \pm .07$
	$0.60 \pm .13$	$0.58 \pm .04$	$0.17 \pm .06$	$0.09 \pm .08$
$T_2$	$6431$ °K	$6431$ °K	$6424$ °K	$6411$ °K
	$6338 \pm 47$ °K	$6140 \pm 36$ °K	$5991 \pm 47$ °K	$6271 \pm 43$ °K
$A$	$1.10 \pm .21$	$1.36 \pm .15$	$1.94 \pm .24$	$-1.93 \pm .24$
	$0.33 \pm .34$	$-0.29 \pm .17$	$-0.16 \pm .22$	$-2.48 \pm .22$
$\Omega$	$4.736 \pm .026$	...	...	...
	$4.741 \pm .023$	...	...	...
$M_2/M_1$	$1.662 \pm .015$	...	...	...
	$1.678 \pm .018$	...	...	...
$\sum wr^2$	.009943	.010240	.015524	.056564
	.009441	.008765	.013732	.055299
$L_1(V)$	$0.3795 \pm .0031$	$0.3786 \pm .0017$	$0.3808 \pm .0027$	$0.3836 \pm .0032$
$(L_1 + L_2)$	$.3931 \pm .0120$	$.4269 \pm .0082$	$.4536 \pm .0116$	$.4048 \pm .0081$
$L_1(B)$	$0.3783 \pm .0036$	$0.3773 \pm .0020$	$0.3797 \pm .0033$	—
$(L_1 + L_2)$	$.3954 \pm .0146$	$.4380 \pm .0103$	$.4714 \pm .0148$	—
$L_1(U)$	$0.3769 \pm .0041$	—	—	—
$(L_1 + L_2)$	$.3983 \pm .0176$	—	—	—
$L_1(4870)$	$0.3789 \pm .0034$	—	—	—
$(L_1 + L_2)$	$.3942 \pm .0133$	—	—	—
$L_1(4110)$	$0.3779 \pm .0039$	—	—	—
$(L_1 + L_2)$	$.3961 \pm .0154$	—	—	—

<sup>a)</sup> Where two entries are given, the upper is for the mode 1 solution, the lower for the mode 3 solution.

Here  $i$  is the inclination of the orbit,  $g$  the gravity darkening exponent,  $T_2$  the polar temperature of the secondary component,  $A$  the bolometric albedo,  $\Omega$  the Roche modified potential at the surface of the system,  $M_2/M_1$  the mass ratio,  $\sum w r^2$  the sum of the weighted squares of the residuals, and  $L_1/(L_1 + L_2)$  the luminosity contribution of component 1 in the five pass bands.

fixed at the values found for epoch I and solved only for the “photometric” quantities  $g$ ,  $A$  and  $L_1$ . Solutions for epochs I, II and III were made from normal points of 4 observations each. Solutions for epoch IV were from the individual observations.

In the normal differential corrections process for TX Cnc we at first encountered a failure of the iterations to converge to small corrections. This problem does not occur for most binaries and an investigation was needed to uncover the cause. Numerous possible sources of the problem were ruled out, and in fact one can show that it cannot be due to any single cause. Rather, convergence is prevented by two difficulties acting together. These are

- 1) high correlations among parameters, and
- 2) neglect of second and, perhaps, higher derivative terms in the equation of condition (cf. Wilson and Devinney, 1971, p. 608).

Since 1) is inherent to the problem and 2) would be prohibitively difficult (in terms of programming and computer time) to correct, we developed a scheme which ensures convergence without loss of rigor, and which requires no programming changes. It is based on the fact that, as experience shows, convergence is adversely affected not so much by a few very high correlations as by the presence of many high correlations

in the matrix of correlation coefficients. Therefore the obvious remedy is to break the large, full parameter set into two or more subsets. For example partition the set  $a, b, c, d, e, f$  into subsets  $A$  ( $a, b, c$ ) and  $B$  ( $d, e, f$ ). Then solve for parameter subsets  $A, B$  alternately, keeping parameters  $d, e, f$  fixed in the  $A$  solutions and  $a, b, c$  fixed in the  $B$  solutions. Schematically these iterations might be represented as

$A \rightarrow B \rightarrow A \rightarrow B \rightarrow A$ , etc.,

with the output from  $A$  being the input to  $B$ , and vice versa. One finds in this way an enormous improvement in convergence, with the only expense being a doubling of the number of computer runs. In fact, total computing time is unaffected or slightly reduced because the individual runs are shorter. Should some concern develop as to whether the solution achieved is unique, one can always start from a different point in parameter space. In our experience, for TX Cnc and other cases, the solutions have always been unique. One minor problem remains. The probable errors computed by standard least squares procedures for the subsets will be unrealistically small because they do not account for correlations with parameters in the other subset. However since the probable errors are insensitive to precise parameter values, one may, for practical pur-

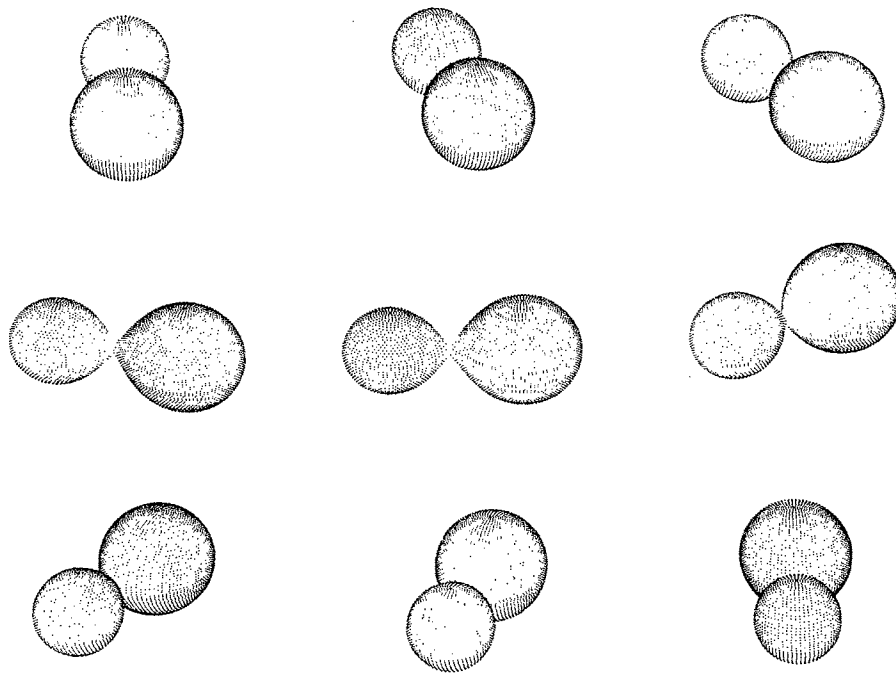


Fig. 6. Computer generated "pictures" of TX Cnc at phases 0.00, 0.05, 0.10, 0.20, 0.25, 0.35, 0.40, 0.45 and 0.50, corresponding to our mode 1 solutions. Notice the small degree of geometrical over-contact

poses, adopt the probable errors given by the last iteration for the full parameter set  $[a, b, c, d, e, f]$  or even make a special final iteration for the entire set, from which only the computed probable errors (not the correlations) will be used. These two procedures are essentially equivalent.

The final parameter values and their probable errors are listed in Table 4. We also computed absolute masses and dimensions, incorporating the spectroscopic results by WWM, but these are so close to those given by WWM that we have not listed them. These absolute masses and dimensions disagree with those given by Yamasaki and Kitamura (1972), which are based on different spectroscopic observations. Figure 6 shows computer generated "pictures" of TX Cnc at several phases, according to the final mode 1 solutions.

We can now inspect Table 4 to see if the epoch-to-epoch changes in  $g$  and  $A$  are in intuitive accord with the epoch-to-epoch changes visible in Figs. 2–5. Comparison of epochs I and II shows no significant changes in  $g$  or  $A$ . This is not surprising because the graphs for epochs I and II are very similar, with the only exception being a slight difference in depth at the very bottom of secondary eclipse. In fact, at the beginning we considered combining epochs I and II. They were separated to see if the least squares process would show significant differences, and it did not. If we compare the epoch I and III light curves we see that the overall amplitude differs by a few hundredths of a magnitude, with III smaller. Table 4 shows that  $g$  is smaller and  $A$  larger in epoch III, mode 1. Since the effects of both smaller  $g$  and larger  $A$  reduce the photometric ellipsoidal variation, we then expect a smaller amplitude of varia-

tion, as observed. The situation is more complicated in the epoch III, mode 3 solution, where  $g$  and  $A$  are both smaller. Detailed comment on this case probably is not warranted. Naturally one should keep in mind that time dependent changes in such quantities as  $g$  and  $A$  may actually be providing information on star spots and similar phenomena rather than gravity darkening and albedo.

The epoch IV light curve is decidedly unlike any ever observed for any other contact binary. A comparison of the observations with the solution curve in Fig. 5 clearly illustrates their strange nature. Evidently WWM observed this unusual WUMa system at a time of particularly unusual behavior—perhaps at a transition between two quasi-equilibrium states. However it must be said that a certain "permanent peculiarity" seems to be associated with the bottom of secondary eclipse, since none of our solutions for any epoch in either mode quite represent the run of observations near phase 0.50, nor does the solution by WWM. Because of the peculiarity of epoch IV, it is not clear whether or not any significance should be attached to the "convective" value of the gravity exponent ( $0.32 \pm 0.07$ ) or the formally negative albedo found for this light curve. However if this number shows a real effect of variable  $g$ , oscillations between different degrees of thermal contact are indeed suggested by the data, as proposed by Lucy (1975).

In comparing our Figs. 2–5 with Fig. 3 of WWM, note that their phases differ by half a cycle from ours. This is not true for their Fig. 2, however. Note also that their convention for designating components 1 and 2 is reversed from ours.

#### IV. Discussion

Our results for mass ratio and inclination are very close to those by WWM. The agreement is particularly remarkable in view of the fact that all of the light curves of TX Cnc show asymmetries and transient effects to greater or lesser degree. It thus seems reasonable to conclude that the departures from good fits shown by our Figs. 2–5 and by Fig. 3 of WWM are due to perturbations from a normal contact binary model and not to any shortcomings of the fitting process. This conclusion is emphasized by the particularly strange light curve of epoch IV (Fig. 5). WWM did not solve for a photometric mass ratio, but their spectroscopic value of  $1.61 \pm 0.05$  p.e. is in virtual coincidence with our photometric value of  $1.66 \pm 0.02$ . Their inclination is  $63^\circ 1 \pm 0^\circ 2$  compared to our  $62^\circ 4 \pm 0^\circ 3$ . There is a significant difference in degree of contact, in that they find 21% overcontact against our 5% and 8% in modes 1 and 3, respectively. Since their solutions were similar to our mode 3, the latter figure (8%) is the proper one for comparison. Note that precise agreement is *not* to be expected because the observations treated were not the same in their work and ours, although some of the  $V$  observations were in common. The slight overcontact agrees with the same finding for RZ Comae (Wilson and Devinney, 1973), another W-type system, and for several W-type systems analysed by Lucy (1972)<sup>2</sup>. Our photometric elements are in rough agreement with those by Yamasaki and Kitamura (1972).

The main distinction between the present results and those of WWM lies in the temperature difference between components. However there is no discord between their numbers and ours when the comparison is made with our mode 3, in which the second temperature is a free parameter, as in their approach. Actually direct comparison is not possible because the observations they solved correspond to our epoch II, but our epoch II solution was constrained to agree with epoch I in regard to  $i$ ,  $\Omega$  and  $q$ , while their solution was not. However, a straight average taken from our epochs I and II shows the photometric primary (the mass secondary) to be hotter by  $173 \pm 35$  °K, in approximate agreement with WWM, who find it hotter by  $125 \pm 10$  °K. Now the main object of this paper is to find if the W-type (i.e. occultation primary eclipse) light curves of TX Cnc can be reproduced just as well by a relatively large gravity effect as by a relatively high temperature for the lower mass star. On the basis of Table 4, it is probably reasonable to conclude that TX Cnc is fitted essentially as well in mode 1 ( $\Delta T$  fixed by the gravity field) as in mode 3 ( $\Delta T$  a free parameter). Of course, since mode 3 has one more degree of freedom than mode 1, its solutions must fit the observations *at least as well* as mode 1. Let us first

<sup>2</sup>) An equivalent reference is Lucy (1973).

consider the epoch I solutions, since they are for the full parameter set. Notice that the values of the sum of the squares of the weighted residuals,  $\Sigma wr^2$ , in Table 4 show that the mode 3 solutions are not very much better than those of mode 1, even though  $T2$  is a crucial parameter for bringing eclipse depths into agreement. Certainly one would be unable to discern, by visual inspection, any difference in the quality of fit between modes 1 and 3, for epoch I. In other words, the degree of freedom provided by  $T2$  adjustment offers only a very marginal or negligible improvement. For epochs II and III, there is a sensible reduction in  $\Sigma wr^2$  in mode 3, and one can actually see a slight improvement in the fit by eye inspection of the appropriate graphs (not shown in Figs. 2–5). However one must remember that  $i$ ,  $\Omega$  and  $q$  were not allowed to adjust at epochs II and III, so that  $T2$  is one of the few parameters available to respond to any transient effects. To illustrate this point by an extreme example, suppose our two cases (i.e. mode 1 and 3 solutions) consisted of adjusting no parameter at all (mode 1) or  $T2$  only (mode 3). Obviously, the mode 1 solution, having no degrees of freedom, would be unable to improve the starting solution, while the mode 3 solution might be expected to effect a noticeable improvement—not because a real correction in  $T2$  was in order, but because  $T2$  was able to mimic the effects of other parameters. Thus it seems best to judge the significance of including  $T2$  by means of the epoch I solutions, which included the full set of parameters.

If one cannot decide between the hypotheses of a hotter lower mass star and relatively large gravity darkening on the basis of the fit to the light curves, how can one decide? Of course, the gravity darkening explanation is simpler, due to having one fewer parameter, and might be preferred for that reason. However one further criterion does exist. This considers the agreement, or lack of agreement, between the derived values of the gravity darkening and albedo parameters and the theoretically predicted values. Unfortunately it is not so clear what theoretical values should be assumed, since essentially classical values are advocated by some and “convective” values by others (Lucy, 1967; Rucinski, 1969). However the situation is not too bad, since we have only two values of each parameter to be recognized<sup>3</sup>). That is,  $g$  should be either 1.0 (classical) or about 0.3 (convective) and  $A$  should be either 1.0 (classical) or about 0.5 (convective). Inspecting the mode 3 results in Table 3 for consistency in  $g$  and  $A$ , we find no clear pattern, in that  $g$  and  $A$  are not consistently near to either the classical or the convective values. For mode 1, however, epochs I and II show a high degree of self-consistency in that both the gravity and albedo

<sup>3</sup>) Smith and Worley (1974) show that  $g$  can have nearly arbitrary values for suitably chosen laws of differential rotation and radiative atmospheres. However, they did not calculate an albedo, so that no comparison can be made here.

parameters are close to the classical values. Epoch IV, which is strikingly different from a normal W UMa-type light curve, and Epoch III, which is very asymmetrical, do not show this consistency and perhaps should be regarded as perturbed epochs. Thus none of the four epochs is consistent with either classical or “convective” theory under mode 3 analysis, but at least the two most normal appearing epochs are in excellent agreement with classical theory under mode 1 analysis. This seems to be a valid reason to prefer mode 1, in which the W-type light curve is explained by TX Cnc having the relatively large von Zeipel gravity darkening and unity albedo. As shown by Tables 3 and 4, the lower mass star (component 1) is then about 25 to 35 °K cooler at its poles than is its companion.

Naturally we do not claim that *no* W type W UMa stars are to be found with hotter lower mass components. Perhaps in their oscillations these systems have hotter (mass) secondaries for intervals of time. However we note that the only two systems (RZ Com and TX Cnc) which have been analysed from a “mode 1” approach have yielded good consistent solutions. Therefore one might expect this to happen for many or even most other W-type light curves, and that the secondaries are *not*, in general, the hotter components, but rather the cooler components. We thus conclude that the observations analysed to date do not provide evidence for different entropy constants in the two convective zones.

*Acknowledgements.* R.E.W. wishes to thank the U.S. National Academy of Sciences—National Research Council for a Senior Research Associateship, which provided his full support at the Goddard Institute for Space Studies while this work was in progress. P.B. wishes to thank the Max-Kade Foundation and the Deutsche Forschungsgemeinschaft (Bi 191/1) for making his stay in New York possible, and the Department of Astronomy at Columbia University for their hospitality; most of this work was carried out while he was in

New York. It was finished while he was at the Universitätssternwarte Göttingen and Astronomische Institute Universität Bonn. We thank Dr. John Whelan for sending the epoch IV observations of TX Cnc.

## References

- Biermann, P., Thomas, H.-C. 1973, *Astron. & Astrophys.* **23**, 55  
 Carbon, D.F., Gingerich, O. 1969, in *Theory and Observation of Normal Stellar Atmospheres*, ed. O. Gingerich, Cambridge, Mass.: MIT Press  
 Haffner, H. 1937, *Z. Astrophys.* **14**, 285  
 Hazlehurst, J. 1970, *Monthly Notices Roy. Astron. Soc.* **149**, 129  
 Kitamura, M., Yamasaki, A. 1971, *Tokyo Astron. Bull.* no. 209  
 Kopal, Z. 1959, *Close Binary Systems*, New York: Wiley  
 Lucy, L.B. 1967, *Z. Astrophys.* **65**, 89  
 Lucy, L.B. 1968 a, *Astrophys. J.* **151**, 1123  
 Lucy, L.B. 1968 b, *Astrophys. J.* **153**, 877  
 Lucy, L.B. 1972, *Proceedings I.A.U. Colloquium 16*  
 Lucy, L.B. 1973, *Astrophys. Space Sci.* **22**, 381  
 Lucy, L.B. 1975, preprint  
 Rucinski, S. 1969, *Acta Astron.* **19**, 245  
 Smith, R.C., Worley, R. 1974, *Monthly Notices Roy. Astron. Soc.* **167**, 199  
 Whelan, J.A.J. 1972, *Monthly Notices Roy. Astron. Soc.* **156**, 115  
 Whelan, J.A.J., Worden, S.P., Mochnacki, S.W. 1973, *Astrophys. J.* **183**, 133  
 Wilson, R.E., Devinney, E.J. 1971, *Astrophys. J.* **166**, 605  
 Wilson, R.E., Devinney, E.J. 1973, *Astrophys. J.* **182**, 539  
 Wilson, R.E., DeLuccia, M.R., Johnston, K., Mango, S.A. 1972, *Astrophys. J.* **177**, 191  
 Yamasaki, A., Kitamura, M. 1972, *Publ. Astron. Soc. Japan* **24**, 213
- R. E. Wilson  
 Department of Astronomy  
 University of South Florida  
 Tampa, Florida 33620, USA
- P. Biermann  
 Astronomische Institute  
 der Universität Bonn  
 Auf dem Hügel 71  
 D-5300 Bonn  
 Federal Republic of Germany